Supplemental Material for "Coexistence of Zero-Dimensional Electride State and Superconductivity in AlH_2 Monolayer"

Qiuping Yang(杨秋萍)[1], Xue Jiang(蒋雪)[1*], and Jijun Zhao(赵纪军)[1*]

[1] *Key Laboratory of Materials Modification by Laser, Ion and Electron Beams (Dalian University of Technology), Ministry of Education, Dalian 116024, China*

[*]Corresponding Author: Email: jiangx@dlut.edu.cn; zhaojj@dlut.edu.cn

1. Computational Details

We used the combination of Al and H elements to fix their stoichiometric ratio of 1:2, and several typical compounds with 1:2 stoichiometries were re-examined in the AlH_2 monolayer by substitutional screening calculations at ambient pressure (Fig. S1). The structural relaxation and electronic properties were performed in the framework of the density functional theory (DFT)[1] within the generalized gradient approximation (GGA)[2] as implemented in the Vienna Ab initio Simulation Package (VASP) code[3,4], using the Perdew-Burke-Ernzerhof (PBE) exchange-correlation functional[2] within the generalized gradient approximation (GGA)[5,6]. The electron projection augmented wave (PAW) method was used to describe electron-ion interaction potentials[7]. The vacuum space of larger than 15 Å was added to avoid the interactions between the layer and its periodic images along the *c*-axis. DFT-D3 method was used to describe long-range van-der-Waals interactions[8]. The plane-wave basis with a

kinetic energy cutoff of 600 eV and the Monkhorst-Pack scheme[9] with a dense *k*-point grid spacing of $2\pi \times 0.03$ $\mathbf{\AA^{-1}}$ were chosen to ensure good convergence of the total energy. To determine the dynamical stability of AlH_2 structures, phonon calculations were performed by using the finite displacement approach[10] as implemented in the Phonopy code[11]. After systematic screening, we have successfully identified a dynamically stable AlH_2 monolayer with *P*-6*m*2 symmetry (Fig. S1d), and the discussion of *P*-6*m*2 AlH_2 monolayer can be found in the main text.

Electron-phonon coupling calculations were carried out as implemented in the QUANTUM ESPRESSO package[12]. We employ the ultrasoft pseudopotentials with $1s^1$ and $3s^2 3p^1$ as valence electrons for Al and H atoms, respectively. The pseudopotential names are Al.pbe-mt_fhi.UPF and H.pbe-rrkjus.UPF. The kinetic energy cutoff for the wave-function expansion was chosen as 60 Ry. To reliably calculate electron-phonon coupling in metallic systems, we need to sample dense *k*-meshes of the electronic Brillouin zone integration and enough *q*-meshes for evaluating average contributions from the phonon modes. We have used a 24 × 24 × 1 *k*-mesh and 12 × 12 × 1 *q*-mesh for calculating the superconducting T_c of 1H-AlH_2 monolayer, which is estimated within the McMillan-Allen-Dynes approximation[13–15]:

$$T_c = \frac{\omega_{\log}}{1.2} \exp\left[-\frac{1.04(1+\lambda)}{\lambda - \mu^*(1+0.62\lambda)} \right]$$

Here, k_B is the Boltzmann constant and μ^* is the Coulomb pseudopotential (μ^* = 0.1). The magnitude of the EPC $\lambda_{q,v}$ can be calculated by:

$$\lambda_{q,v} = \frac{\gamma_{q,v}}{\pi h N(E_F)\omega_{q,v}{}^2}$$

where $\gamma_{q,v}$ is the phonon linewidth, $N(E_F)$ is the electronic density of states at the Fermi level, and the $\omega_{q,v}$ is the phonon frequency. The phonon linewidths $\gamma_{q,v}$ can be estimated by

$$\lambda_{q,v} = \frac{2\pi\omega_{qv}}{\Omega_{BZ}} \sum_{k,n,m} \left| g^{v}_{kn,k+qm} \right|^2 \delta(\varepsilon_{k,n} - \varepsilon_F)\delta(\varepsilon_{k+qm} - \varepsilon_F)$$

where $\left| g^{v}_{kn,k+qm} \right|$ is the electron-phonon matrix element between two electronic states with momenta k and k + q at the Fermi level.

$$\mathrm{g}^{v}_{kn,k+qm}(k,q) = \left(\frac{\hbar}{2M\omega_{q,v}}\right)^{\frac{1}{2}} \left\langle n,k \left| \delta V^{q,v}_{scf} \right| m,k+q \right\rangle$$

The Eliashberg spectral function for the electron-phonon interaction and the frequency-dependent EPC can be calculated as follows:

$$\alpha^2 F(\omega) = \frac{1}{2\pi N(E_F)} \sum_{q,v} \frac{\gamma_{q,v}}{\omega_{q,v}} \delta(\omega - \omega_{q,v})$$

$$\lambda(\omega) = 2\int_0^{\omega} \frac{\alpha^2 F(\omega)}{\omega} d\omega$$

$$\omega_{\log} = \exp\left[\frac{2}{\lambda} \int \frac{d\omega}{\omega} \alpha^2 F(\omega) \ln(\omega) \right]$$

Anisotropic superconducting properties have been investigated by solving the fully anisotropic Migdal-Eliashberg equations as implemented in the electron-phonon Wannier (EPW) code[16–18]. The precedent computations

of the electronic wave functions required for the Wannier interpolations are performed in a uniform unshifted BZ *k*-mesh of 12 × 12 × 1. An interpolated *k*-point grid of 240 × 240 × 1 and *q*-point grid of 120 × 120 ×1 are used to solve the anisotropic Migdal-Eliashberg equations. The fermion Matsubara frequencies cutoff is set to 1.2 eV, a reasonable setting is 4 times higher than the largest phonon frequency. The Morel-Anderson pseudopotential μ_c^* is set to 0.13.

Supplemental Figures

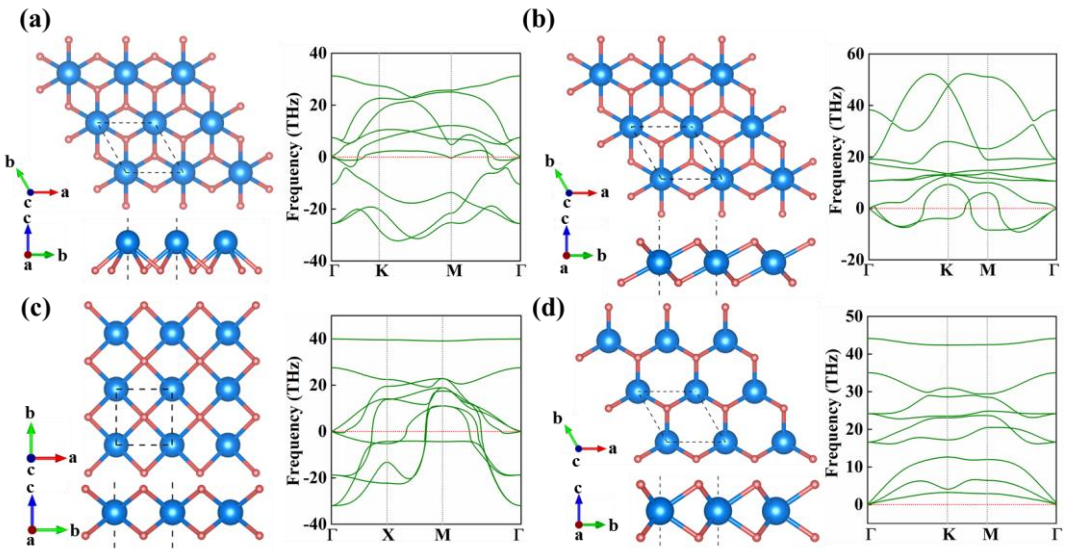

Fig. S1 Optimized structures and phonon dispersion curves of the AlH_2 monolayer with (a) *P*6*mm*, (b) *P*-3*m*1, (c) *P*4/*mmm,* and (d) *P*-6*m*2 symmetry.

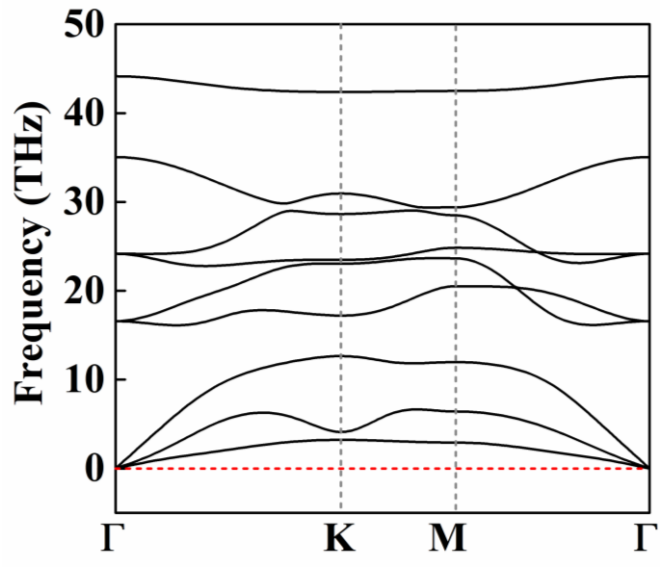

Fig. S2 Phonon dispersion curves of 1H-AlH_2 monolayer.

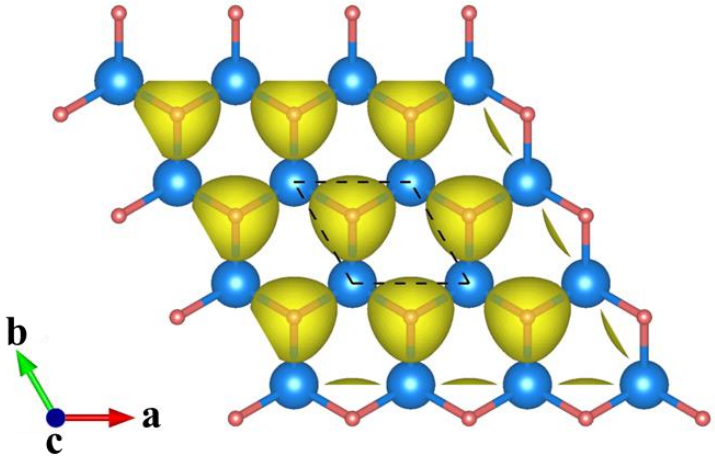

Fig. S3 Electron localization function (ELF) of a hypothetical structure $[AlH_2]^+$ by removing one electron per formula unit from 1H-AlH_2 monolayer.

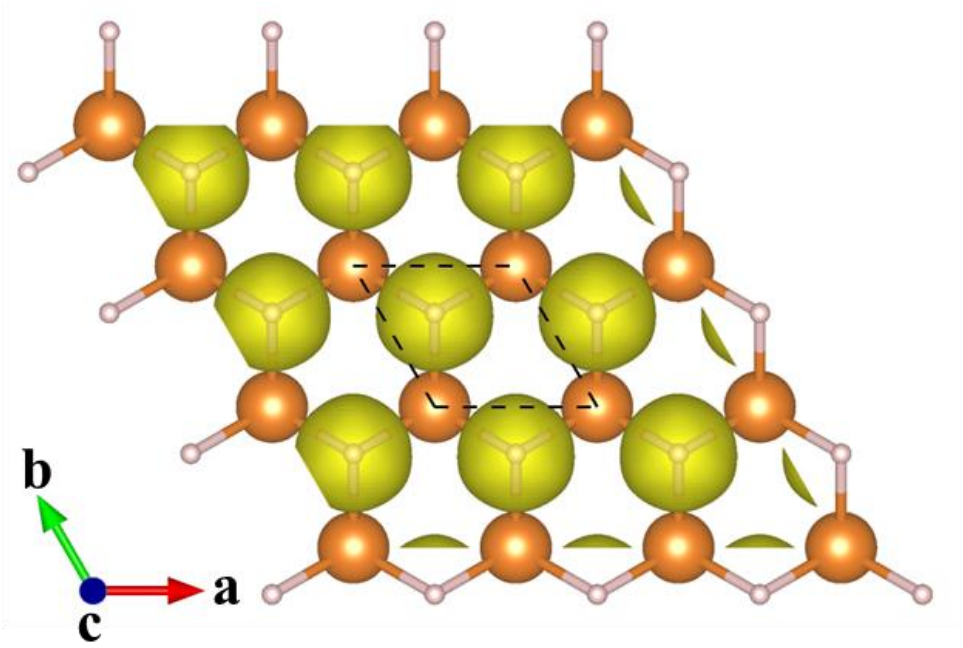

Fig. S4 Electron localization function (ELF) of MgH_2 monolayer.

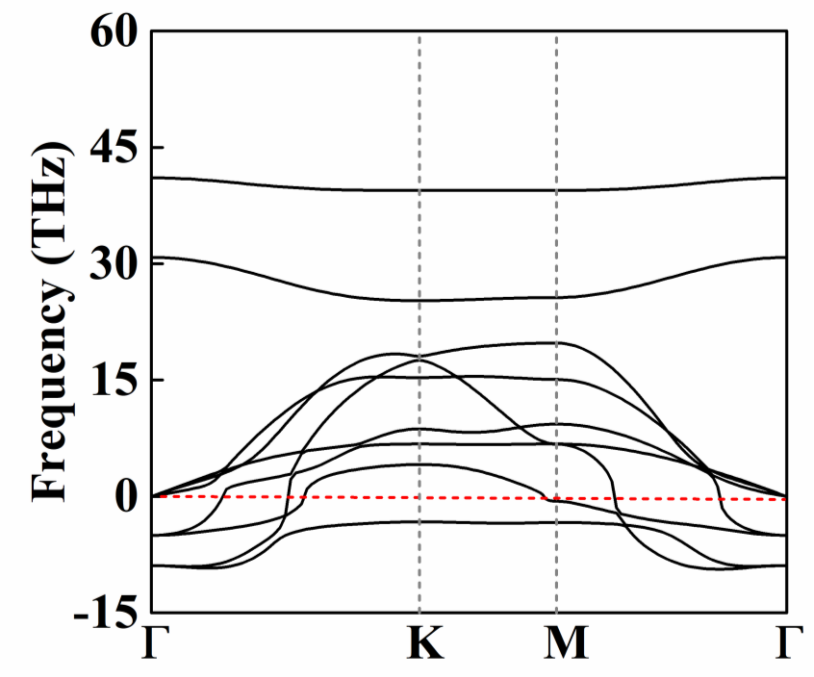

Fig. S5 Phonon dispersion curves of MgH_2 monolayer.

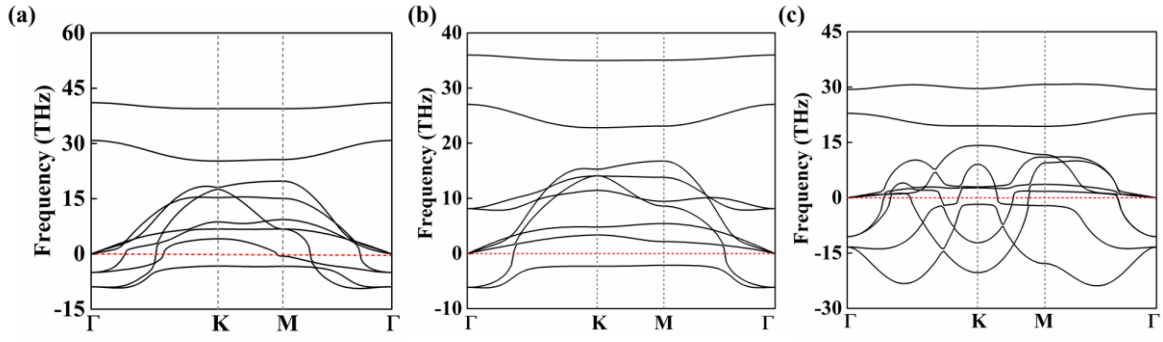

Fig. S6 Phonon dispersion curves of GaH_2, InH_2 and TlH_2 monolayers.

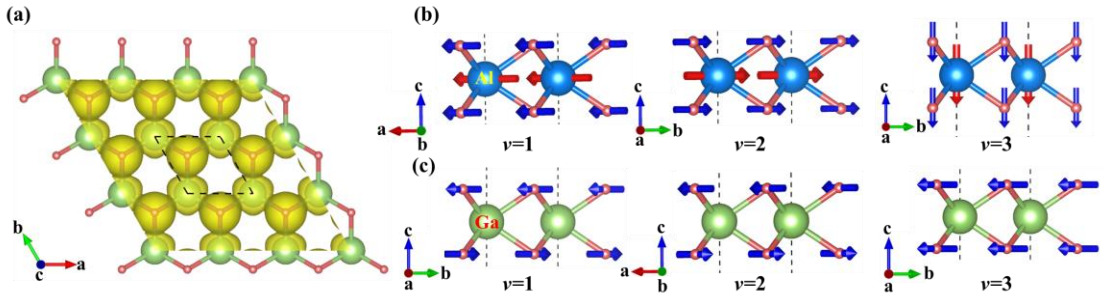

Fig. S7 (a) Electron localization function (ELF) of MgH_2 monolayer. (b) The acoustic vibrational modes of 1H-AlH_2 and GaH_2 monolayers at Γ point in the Brillouin zone (The arrows represent the direction of atomic vibration).

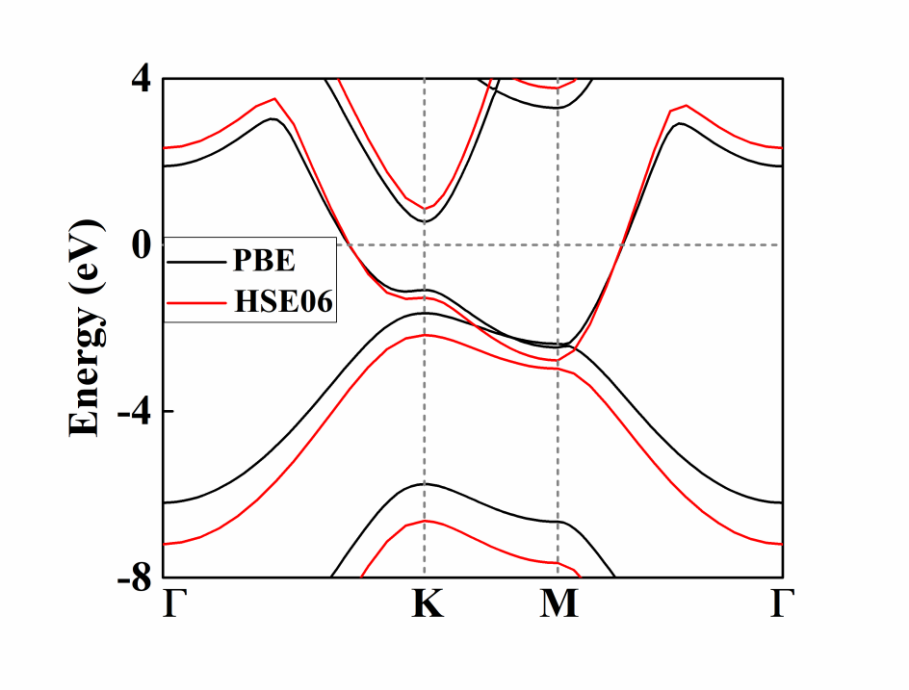

Fig. S8 Electronic band structures of the 1H-AlH_2 monolayer at the PBE (black) and HSE06 (red) levels. The metallicity is also verified using the HSE06 functional.

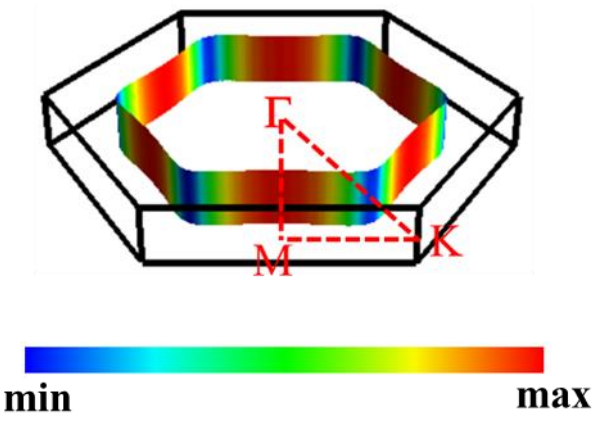

Fig. S9 Fermi surface corresponding to the one band crossing the Fermi level, color-coded by the Fermi velocity.

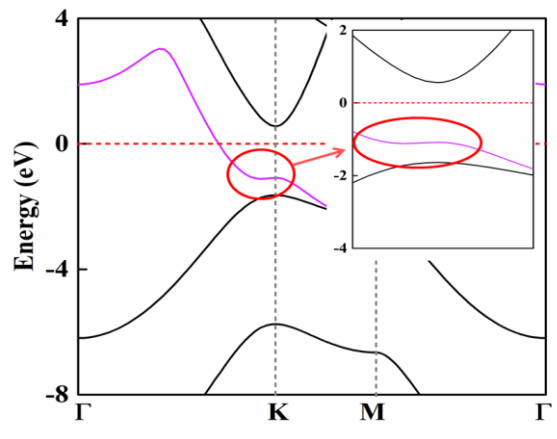

Fig. S10 Electronic band structure of 1H-AlH_2 monolayer calculated at the PBE level. An enlarged plot of the flat bands near the Fermi level is shown in inset.

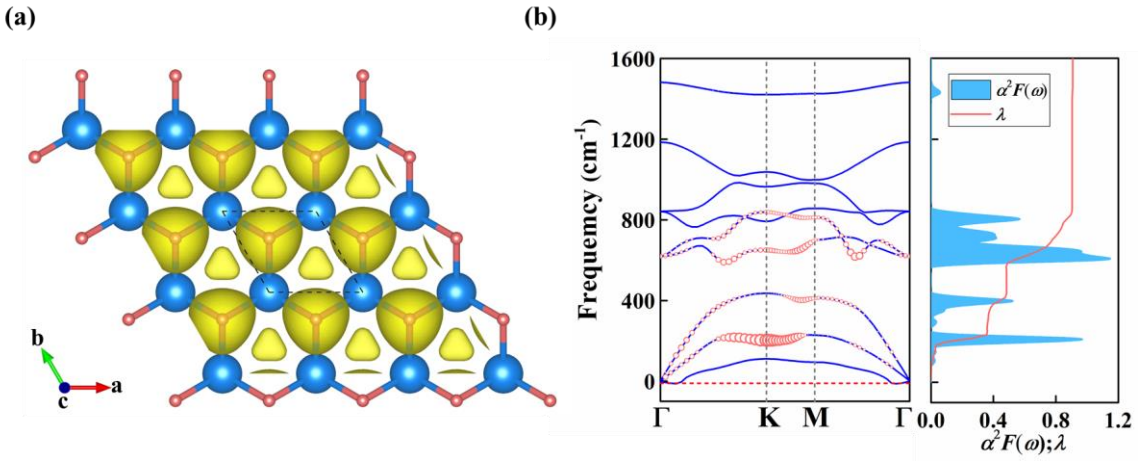

Fig. S11 (a) Electron localization function (ELF) of 1H-AlH_2 monolayer under biaxial compressive strain of 1%. (b) Eliashberg spectral function (blue area) and frequency-dependent EPC parameter λ (red line) of the 1H-AlH_2 monolayer under 1% compressive strain of. The size of red circles in the phonon spectra is proportional to partial EPC parameter $\lambda_{q,v}$. Using a typical Coulomb pseudopotential parameter of μ*=0.1, the resulting T_c is 33 K.

Supplemental Tables

Table S1. Structural information of 1H-AlH_2 monolayer.

Space group	Lattice parameters	Atomic coordinates			
		Atoms	*x*	*y*	*z*
P-6*m*2	*a*=2.720 Å *b*=2.720 Å *c*=17.052 Å *α*=*β*=90° *γ*=120°	Al(1*b*)	0.0000	0.0000	0.50000
		H (2*h*)	0.3333	0.6667	0.43692

References

[1] Kohn W and Sham L J 1965 *Phys. Rev.* **140** A1133–8

[2] Perdew J P, Burke K and Ernzerhof M 1996 *Phys. Rev. Lett.* **77** 3865–8

[3] Kresse G and Joubert D 1999 *Phys. Rev. B* **59** 1758–75

[4] Kresse G and Furthmüller J 1996 *Phys. Rev. B* **54** 11169–86

[5] Lee C, Yang W and Parr R G 1988 *Phys. Rev. B* **37** 785–9

[6] Becke A D 1988 *Phys. Rev. A* **38** 3098–100

[7] Blöchl P E 1994 *Phys. Rev. B* **50** 17953–79

[8] Grimme S, Antony J, Ehrlich S and Krieg H 2010 *J. Chem. Phys.* **132** 154104

[9] Monkhorst H J and Pack J D 1976 *Phys. Rev. B* **13** 5188–92

[10] Parlinski K, Li Z Q and Kawazoe Y 1997 *Phys. Rev. Lett.* **78** 4063–6

[11] Togo A, Oba F and Tanaka I 2008 *Phys. Rev. B* **78** 134106

[12] Giannozzi P, Baroni S, Bonini N, Calandra M, Car R, Cavazzoni C, Ceresoli D, Chiarotti G L, Cococcioni M, Dabo I, Dal Corso A, de Gironcoli S, Fabris S, Fratesi G, Gebauer R, Gerstmann U, Gougoussis C, Kokalj A, Lazzeri M, Martin-Samos L, Marzari N, Mauri F, Mazzarello R, Paolini S, Pasquarello A, Paulatto L, Sbraccia C, Scandolo S, Sclauzero G, Seitsonen A P, Smogunov A, Umari P and Wentzcovitch R M 2009 *J. Phys. Condens. Matter* **21** 395502

[13] Oliveira L N, Gross E K U and Kohn W 1988 *Phys. Rev. Lett.* **60** 2430–3

[14] Lüders M, Marques M A L, Lathiotakis N N, Floris A, Profeta G, Fast L, Continenza A, Massidda S and Gross E K U 2005 *Phys. Rev. B* **72** 24545

[15] Marques M A L, Lüders M, Lathiotakis N N, Profeta G, Floris A, Fast L, Continenza A, Gross E K U and Massidda S 2005 *Phys. Rev. B* **72** 24546

[16] Allen P B and Dynes R C 1975 *Phys. Rev. B* **12** 905–22

[17] Migdal A B 1968 *Sov. Phys. JETP* **35** 996

[18] Poncé S, Margine E R, Verdi C and Giustino F 2016 *Comput. Phys. Commun.* **209** 116–33